

Introduction to RALEF-2D — a two-dimensional radiation-hydrodynamics code

M. M. Basko

ILE, Osaka, December 17, 2010

Equations of hydrodynamics

The newly developed **RALEF-2D** code is based on a one-fluid, one-temperature hydrodynamics model in two spatial dimensions (either x,y, or r,z):

$$\frac{\partial \rho}{\partial t} + \nabla \cdot (\rho \vec{u}) = 0,$$

$$\frac{\partial (\rho \vec{u})}{\partial t} + \nabla \cdot (\rho \vec{u} \otimes \vec{u}) + \nabla p = 0,$$

$$\frac{\partial (\rho E)}{\partial t} + \nabla \cdot [(\rho E + p) \vec{u}] = \nabla \cdot (\kappa \nabla T) + Q_r + Q_{dep},$$

$$E = e + \frac{u^2}{2}, \quad e = e(\rho, T)$$

$\nabla \cdot (\kappa \nabla T)$ – energy deposition by thermal conduction (local), Q_r – energy deposition by radiation (non-local), Q_{dep} – eventual external heat sources.

Radiation transport

Transfer equation for radiation intensity I_ν in the quasi-static approximation:

$$\cancel{\frac{1}{c} \frac{\partial I_\nu}{\partial t}} + \vec{\Omega} \cdot \nabla I_\nu = k_\nu (B_\nu - I_\nu), \quad I_\nu = I_\nu(t, \vec{x}, \nu, \vec{\Omega}), \quad B_\nu = B_\nu(\nu, T)$$

Quasi-static approximation: radiation transports energy infinitely fast (compared to the fluid motion) \Rightarrow the energy residing in radiation field at any given time is infinitely small !

In the present version, the absorption coefficient k_ν and the source function $B_\nu = B_\nu(T)$ are calculated in the LTE approximation.

Coupling with the fluid energy equation:

$$Q_r = -\nabla \cdot \left(\int d\nu \int \vec{\Omega} I_\nu d\vec{\Omega} \right) = \int_{4\pi} d\vec{\Omega} \int k_\nu (I_\nu - B_\nu) d\nu$$

Radiation transport adds 3 extra dimensions (two angles and the photon frequency) \Rightarrow **the 2D hydrodynamics becomes a 5D radiation hydrodynamics !**

New quality due to radiation transport

Pure hydrodynamics (with or without thermal conductivity) is local.

Radiation hydrodynamics is non-local !

- ⇒ poses serious difficulties for the development of adequate numerical algorithms in 2 and 3 dimensions;
- ⇒ **RALEF-2D** is based on a newly developed original algorithm for radiation transport (not published yet).

Main constituents of the RALEF-2D package

- 1. Hydrodynamics**
- 2. Thermal conduction**
- 3. Radiation transport**
- 4. EOS and opacities**
- 5. Laser absorption**

Hydrodynamics

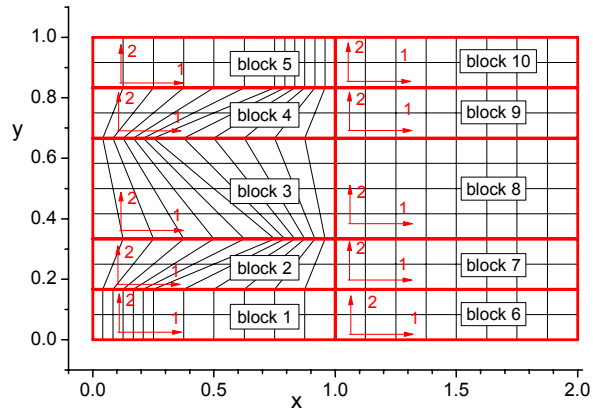
Numerical scheme for hydrodynamics

The numerical scheme for the 2D hydrodynamics is built upon the CAVEAT-2D (LANL, 1990) hydrodynamics package and has the following properties:

- ❖ it uses cell-centered principal variables on a multi-block structured quadrilateral mesh (either in the x-y or r-z geometry);
- ❖ is fully conservative and belongs to the class of second-order Godunov schemes (no artificial viscosity is needed);
- ❖ the mesh is adapted to the hydrodynamic flow by applying the ALE (arbitrary Lagrangian-Eulerian) technique;
- ❖ the numerical method is based on a fast non-iterative Riemann solver (J.K.Dukowicz, 1985), easily applied to arbitrary equation of state.

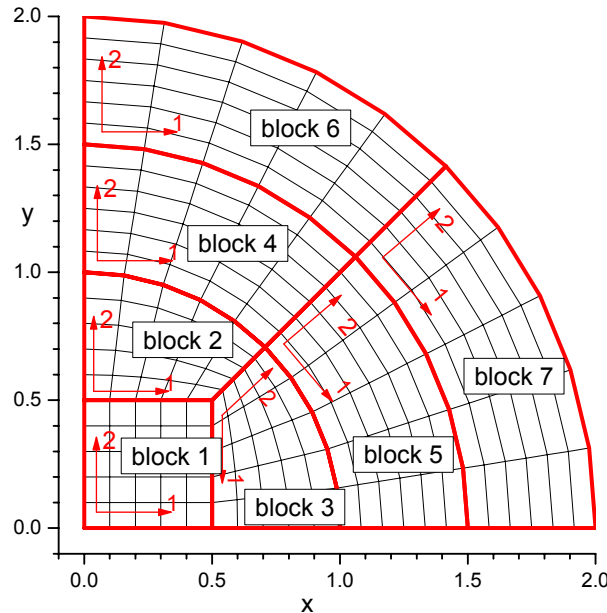
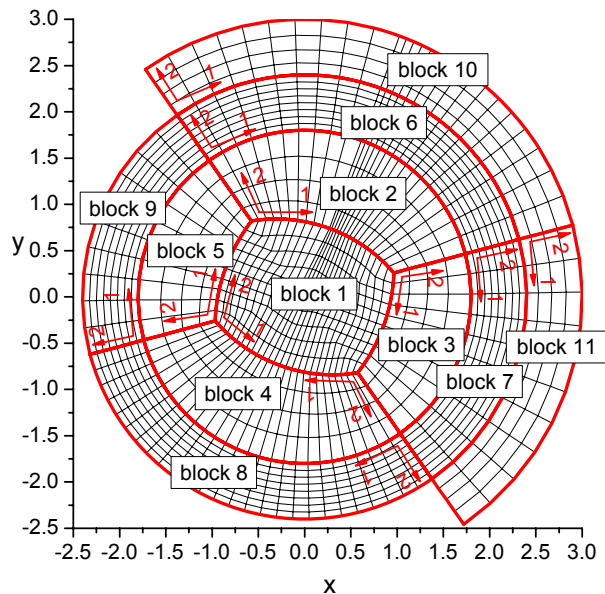
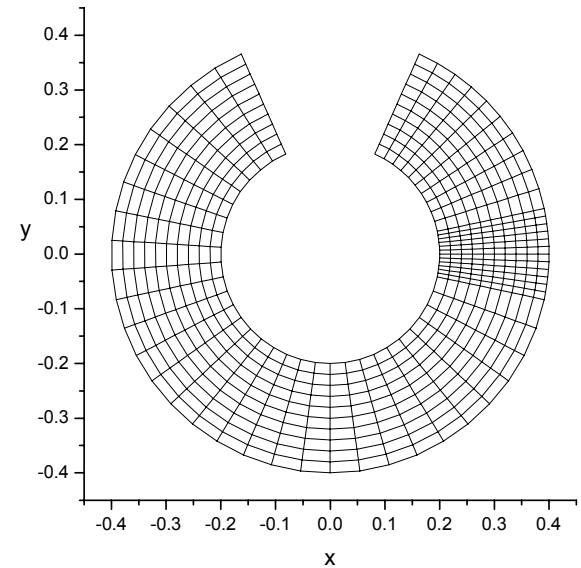
Computational mesh: general topology

Computational mesh consists of blocks with common borders. Each block is topologically equivalent to a rectangle. Common block faces have equal number of cells.



Mesh geometry:

- Cartesian (x,y)
- cylindrical (r,z)

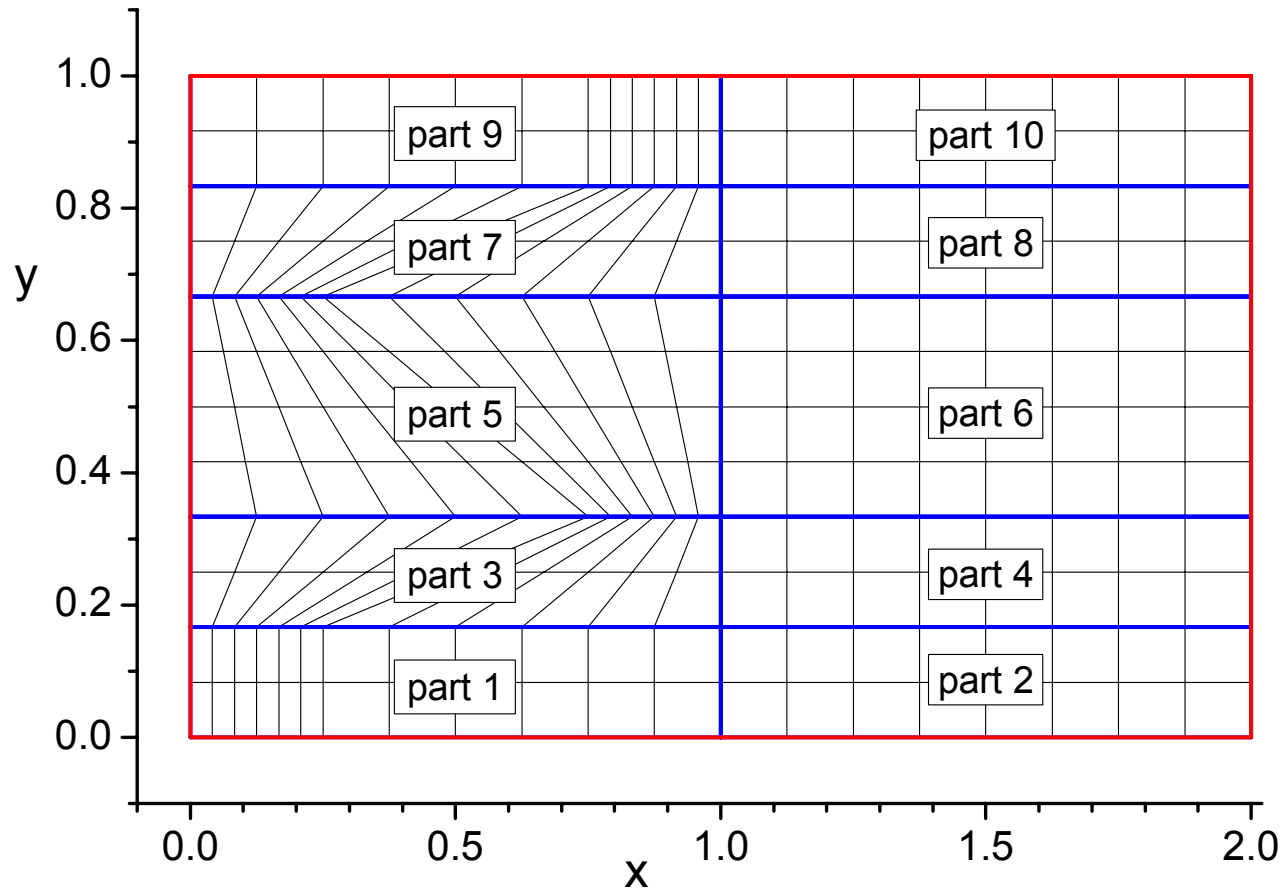


Mesh library:

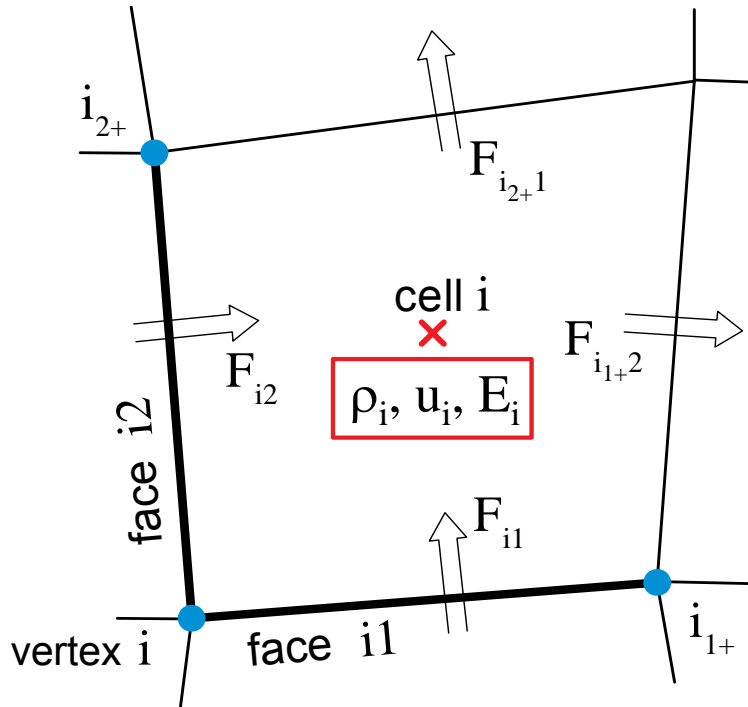
Different mesh options, distinguished by the value of variable **igeom**, are combined into a mesh library, which is being continuously expanded.

Computational mesh: block structure

Every block can be subdivided into $n_{p1} \times n_{p2}$ topologically rectangular parts; different parts can be composed of different materials.



The Godunov numerical method



A fast non-iterative Riemann solver by J.K.Dukowicz (1985) is used.

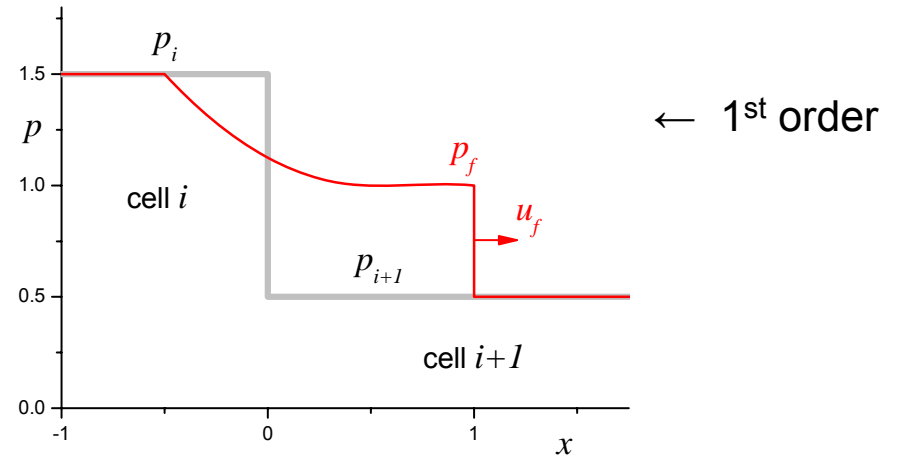
No artificial viscosity is needed !

Principal variables: $\rho, u, E = e + \frac{u^2}{2}$

— all assigned to the cell centers !

Equation of state: $p = p(\rho, e)$

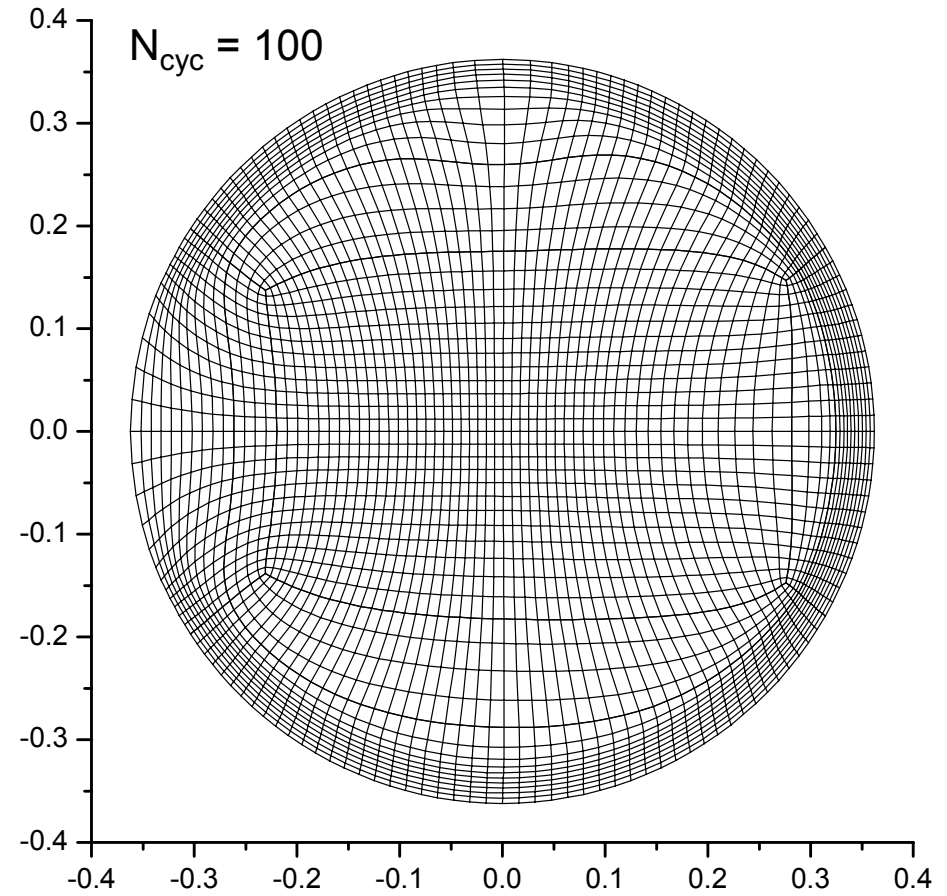
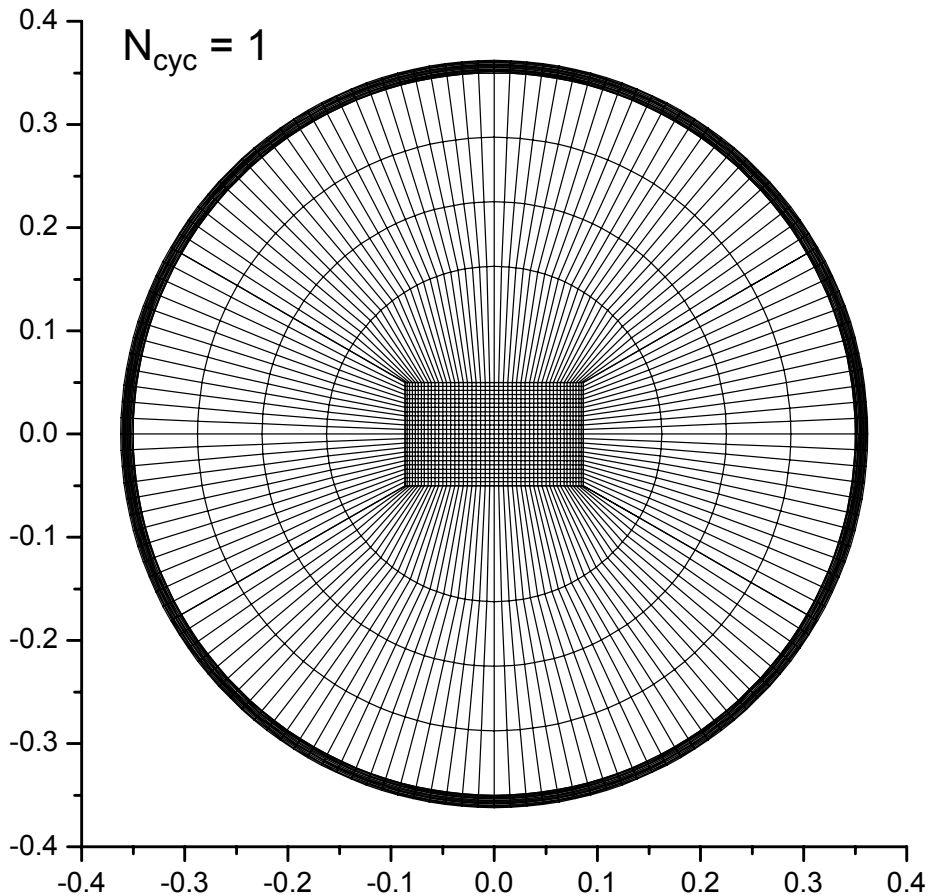
Lagrangian phase: the Riemann problem is solved at each cell face \Rightarrow fluxes F of momentum ρu and total energy E
 \Rightarrow new $u_i(t+dt)$ and $E_i(t+dt)$; mass is conserved.



A "snag": node velocities u_{vi} !

ALE technique

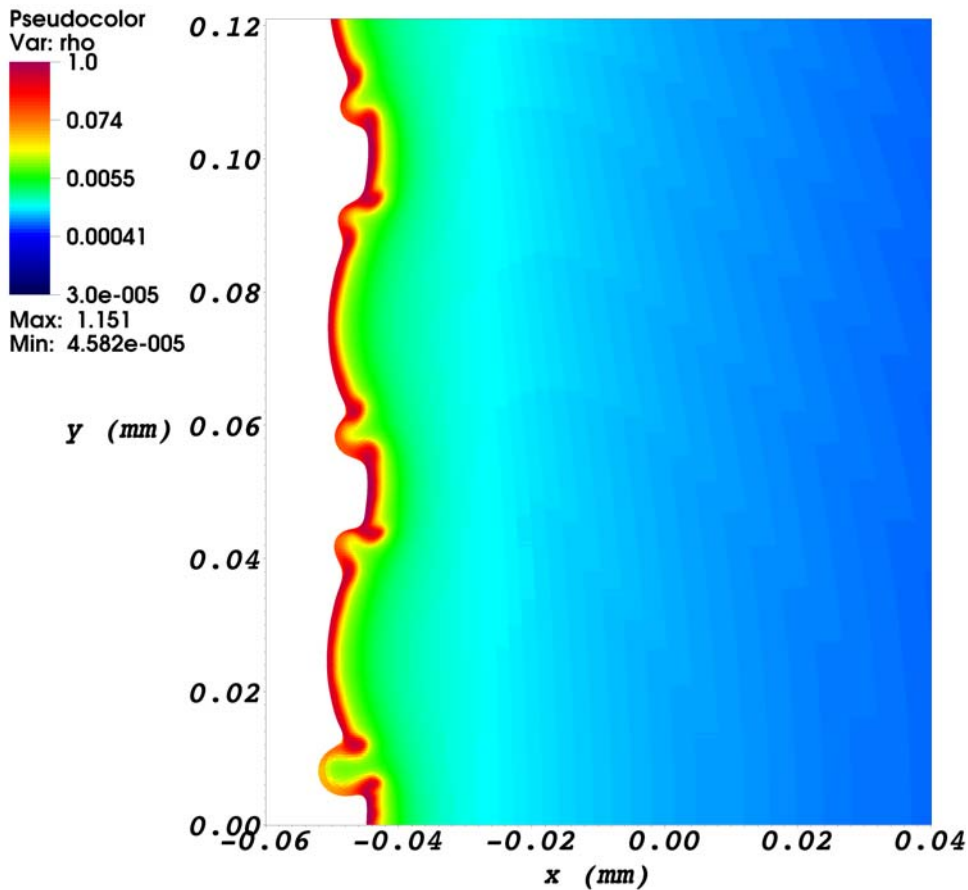
In the arbitrary Lagrangian-Eulerian (ALE) technique, the Lagrangian phase of every hydrocycle is followed by the rezoning (mesh movement) and remapping phases. Material interfaces are traced as Lagrangian surfaces.



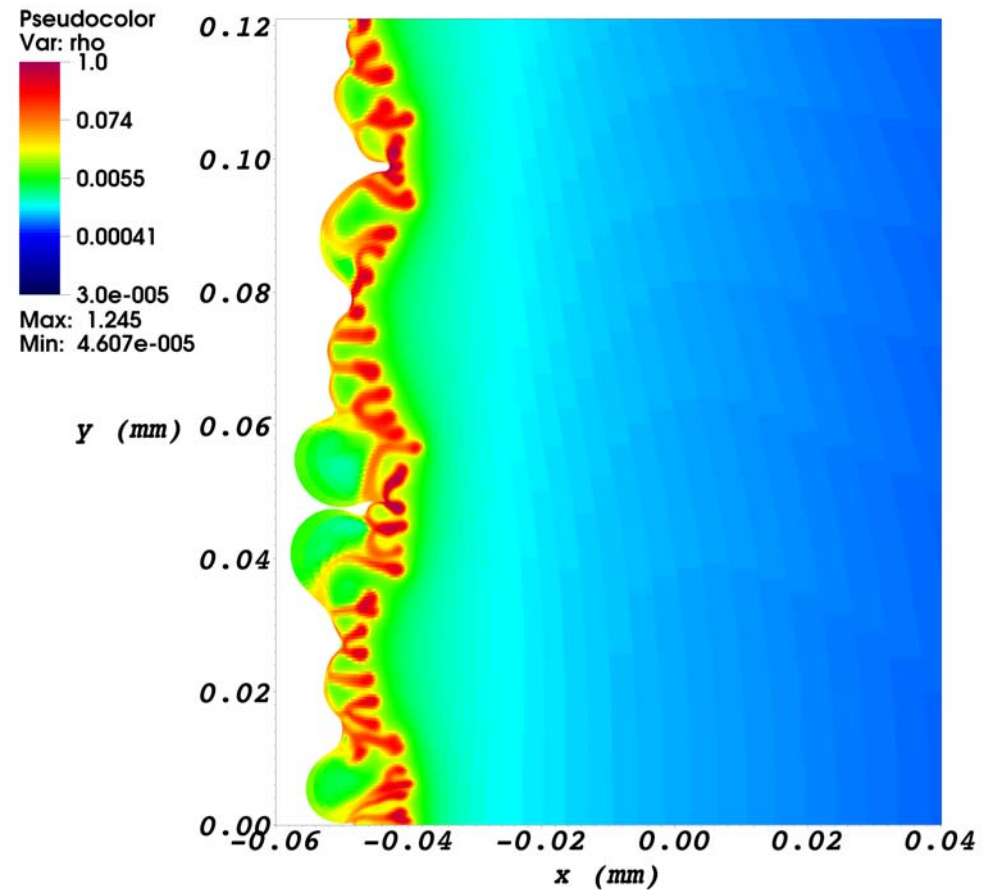
Importance of the 2-nd order + ALE

Non-linear stage of the Rayleigh-Taylor instability of a laser-irradiated thin carbon foil

RALEF: 1-st order



RALEF: 2-nd order



Comparison with KIAM (Moscow)

ЧИСЛЕННОЕ РЕШЕНИЕ
МНОГОМЕРНЫХ
ЗАДАЧ
ГАЗОВОЙ ДИНАМИКИ

Под редакцией С. К. ГОДУНОВА



ИЗДАТЕЛЬСТВО «НАУКА»
ГЛАВНАЯ РЕДАКЦИЯ
ФИЗИКО-МАТЕМАТИЧЕСКОЙ ЛИТЕРАТУРЫ
Москва 1976

For comparison:

At the Keldysh Institute of Applied Mathematics in Moscow a 2D hydrocode, based on the original Godunov method, was developed under the guidance of late Prof. A.V. Zabrodin.

There is a long history of collaboration between ITEP and KIAM on 2D hydro simulations.

Hydrodynamics: comparison with KIAM

KIAM code

1. **Riemann solver**: iterative for a two-term EOS (Zabrodin et al.); accurate for the ideal-gas EOS; slow and capricious for realistic EOS.
2. Only the first order in the Godunov method.
3. Either Lagrangian or Eulerian mesh.

RALEF-2D

1. **Riemann solver**: non-iterative for an arbitrary EOS (J.K.Dukowicz, LANL, 1985); fast and robust for any EOS at the cost of a certain loss of accuracy.
2. More accurate second-order Godunov method.
3. Fully adaptive mesh with an efficient second-order rezoning algorithm [Winslow (LLNL, 1981) + Brackbill (LANL) + Basko (ITEP, 2009)].

Hydrodynamics: comparison with CHIC (CELIA)

CHIC code (CELIA, Bordeaux):

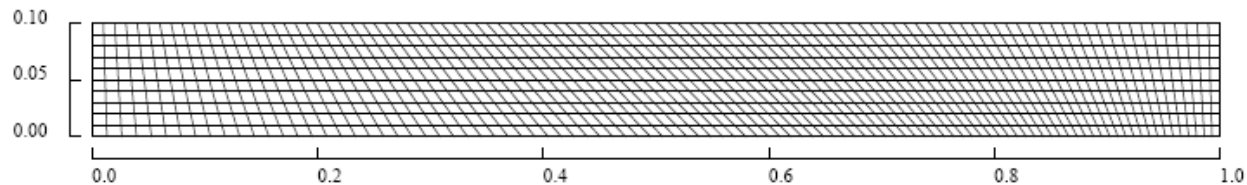
A more complex Riemann solver by P.-H. Maire:

1-st order, acoustic approximation non-iterative (2006) ⇒

⇒ 2-nd order, iterative (2009) [slower than RALEF?] – to be yet benchmarked !

CHIC: succeeds on the Saltzman test (pure Lagrangian mode);

RALEF: fails on the Saltzman test in the Lagrangian mode, runs in the ALE mode.



Hydrodynamics: comparison with MULTI-2D

Computer Physics Communications 180 (2009) 977–994



Contents lists available at ScienceDirect

Computer Physics Communications

www.elsevier.com/locate/cpc



MULTI2D – a computer code for two-dimensional radiation hydrodynamics [☆]

R. Ramis ^{a,*}, J. Meyer-ter-Vehn ^b, J. Ramírez ^a

- ❖ unstructured triangular mesh,
- ❖ an original version of the Lagrangian finite-difference hydrodynamics with artificial viscosity,
- ❖ no ALE.

Thermal conduction

Numerical scheme for thermal conduction

The key ingredient to the RALEF-2D code is the **SSI (symmetric semi-implicit)** method of E.Livne & A.Glasner (1985), used to incorporate **thermal conduction** and **radiation transport** into the 2D Godunov method (in order to avoid costly matrix inversion required by fully implicit methods).

The numerical scheme for thermal conduction (M.Basko, J.Maruhn & A.Tauschwitz, J.Com.Phys., **228**, 2175, 2009) has the following features:

- ❖ it uses cell-centered temperatures from the FVD (finite volume discretization) hydrodynamics on distorted quadrilateral grids,
- ❖ is fully conservative (based on intercellular fluxes with an SSI energy correction for the next time step),
- ❖ (almost) unconditionally stable,
- ❖ space second-order accurate on all grids for smooth κ ,
- ❖ symmetric on a local 9-point stencil,
- ❖ computationally efficient.

Time discretization – the SSI method

For our form of the equation of state: $T = T(\rho, e)$.

Explicit time discretization of the energy equation (Lagrangian form):

$$M_{ij} \left(\bar{E}_{ij} - E_{ij} \right) = \left(W_{ij}^T + W_{ij}^r + W_{ij}^{dep} \right) \Delta t + W_{ij}^p \Delta t$$

Partially-implicit time discretization:

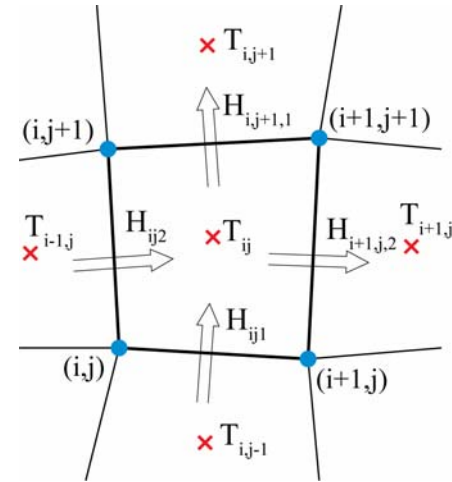
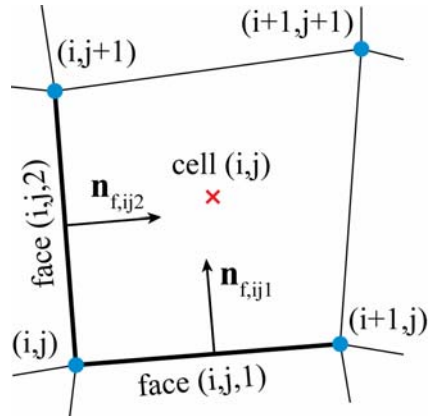
$$M_{ij} \left(\bar{E}_{ij} - E_{ij} \right) = \left(\tilde{W}_{ij}^T + \tilde{W}_{ij}^r + W_{ij}^{dep} \right) \Delta t + W_{ij}^p \Delta t$$

$$c_{V,ij} M_{ij} \left(\tilde{T}_{ij} - T_{ij} \right) = \left(\tilde{W}_{ij}^T + \tilde{W}_{ij}^r + W_{ij}^{dep} \right) \Delta t$$

← equation for \tilde{T}_{ij} solved at the SSI stage

To calculate the partially-implicit cell heating powers $\tilde{W}_i^T + \tilde{W}_i^r$, we use the “new” central temperature \tilde{T}_{ij} , and the “old” side temperatures $T_{i,j+1}$, $T_{i+1,j}$, ... (the SSI proper).

The SSI method for thermal conduction



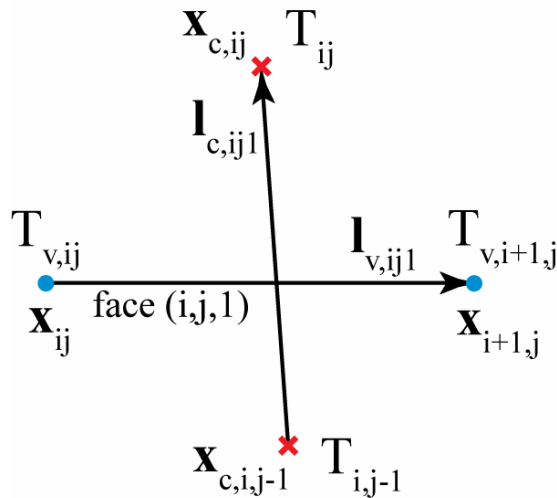
$$\tau_{ij} \equiv \tilde{T}_{ij} - T_{ij} = \frac{(H_{ij1} + H_{ij2} - H_{i,j+1,1} - H_{i+1,j,2} + q_{ij} M_{ij}) \Delta t + \delta_{ij}}{c_{V,ij} M_{ij} + (a_{ij1} + a_{ij2} + b_{i,j+1,1} + b_{i+1,j,2}) \Delta t},$$

$$a_{ijm} = -\frac{\partial H_{ijm}}{\partial T_{ij}} > 0,$$

$$\tilde{\delta}_{ijm} = \Delta t \cdot a_{ijm} \tau_{ij} + \Delta t \cdot b_{ijm} \cdot \begin{cases} \tau_{i,j-1}, & m=1, \\ \tau_{i-1,j}, & m=2, \end{cases}$$

$$b_{ijm} = +\frac{\partial H_{ijm}}{\partial T_{backwd}} > 0.$$

Spatial discretization — the explicit fluxes H_{ijm}



The integrated flux across face (i,j,m) is given by

$$H_{ijm} = -\kappa_{f,ijm} \left(\vec{g}_{f,ijm} \cdot \vec{n}_{f,ijm} \right) \left| \vec{l}_{v,ijm} \right| R,$$

$$\vec{g} = \nabla T;$$

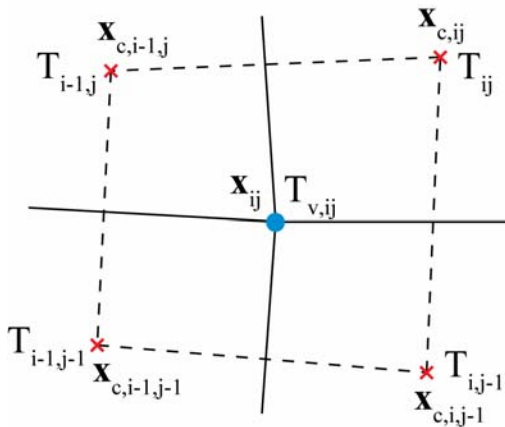
If we assume that we know the vertex temperatures $T_{v,ij}$, the face-centered temperature gradient can be evaluated from an obvious system of two linear equations

$$\begin{cases} \vec{g}_{f,ijm} \cdot \vec{l}_{v,ijm} = \Delta T_{v,ijm} \\ \vec{g}_{f,ijm} \cdot \vec{l}_{c,ijm} = \Delta T_{c,ijm} \end{cases}$$

Generalization to the case of **discontinuous** κ and/or normal component of $\vec{g}_{f,ijm}$ is straightforward.

Vertex temperatures

To close the numerical scheme, we need an interpolation formula for the vertex temperatures. An effective algorithm is based on a bilinear interpolation in “natural” coordinates $(\xi, \eta) \in [-1, +1] \times [-1, +1]$ on a distorted **c-quadrilateral**:



$$\vec{x} = \frac{1}{4} \left[\vec{x}_{c,ij} (1+\xi)(1+\eta) + \vec{x}_{c,i-1,j} (1-\xi)(1+\eta) + \vec{x}_{c,i,j-1} (1+\xi)(1-\eta) + \vec{x}_{c,i-1,j-1} (1-\xi)(1-\eta) \right]$$

$$T(\vec{x}) = \frac{1}{4} \left[T_{c,ij} (1+\xi)(1+\eta) + T_{c,i-1,j} (1-\xi)(1+\eta) + T_{c,i,j-1} (1+\xi)(1-\eta) + T_{c,i-1,j-1} (1-\xi)(1-\eta) \right]$$

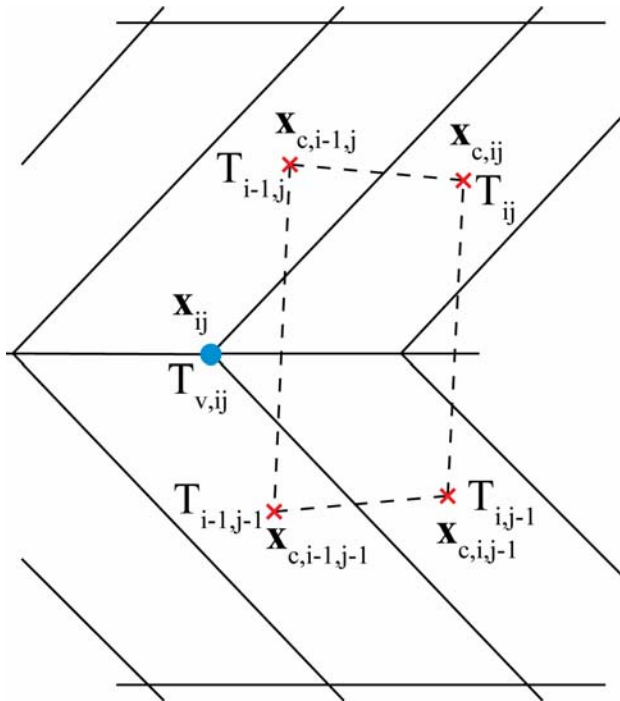
Important property: this interpolation reconstructs exactly an arbitrary linear function

$$T(\vec{x}) = a + \vec{b} \cdot \vec{x}$$

on an arbitrary quadrilateral grid \Rightarrow 2nd order in space !

For discontinuous κ the weights in the second formula are multiplied by κ_{ij} , $\kappa_{i-1,j}$, $\kappa_{i,j-1}$, $\kappa_{i-1,j-1}$.

Strongly distorted grids



On strongly distorted grids the bilinear interpolation becomes non-positive!

To restore positiveness on a logically local stencil, we have to introduce additional constraints, which degrade the spatial convergence order on strongly distorted grids.

Time step control in the SSI method

Constraints on Δt are based on usual approximation-accuracy considerations, but here we need two separate criteria with two control parameters:

$$\left| \frac{\left(H_{ij1} + H_{ij2} - H_{i,j+1,1} - H_{i+1,j,2} + W_{ij}^r + q_{ij} M_{ij} \right) \Delta t}{c_{V,ij} M_{ij} + \left(a_{ij1} + a_{ij2} + b_{i,j+1,1} + b_{i+1,j,2} + D_{ij}^r \right) \Delta t} \right| \leq (\varepsilon_0 - \varepsilon_1) (T_{ij} + T_s),$$

$$\left| \frac{\tilde{\delta}_{ij}}{c_{V,ij} M_{ij}} \right| \leq \varepsilon_1 (T_{ij} + T_s).$$

T_s is a problem-specific sensitivity threshold for temperature variations.

Test problems: linear steady-state solutions

The linear solution

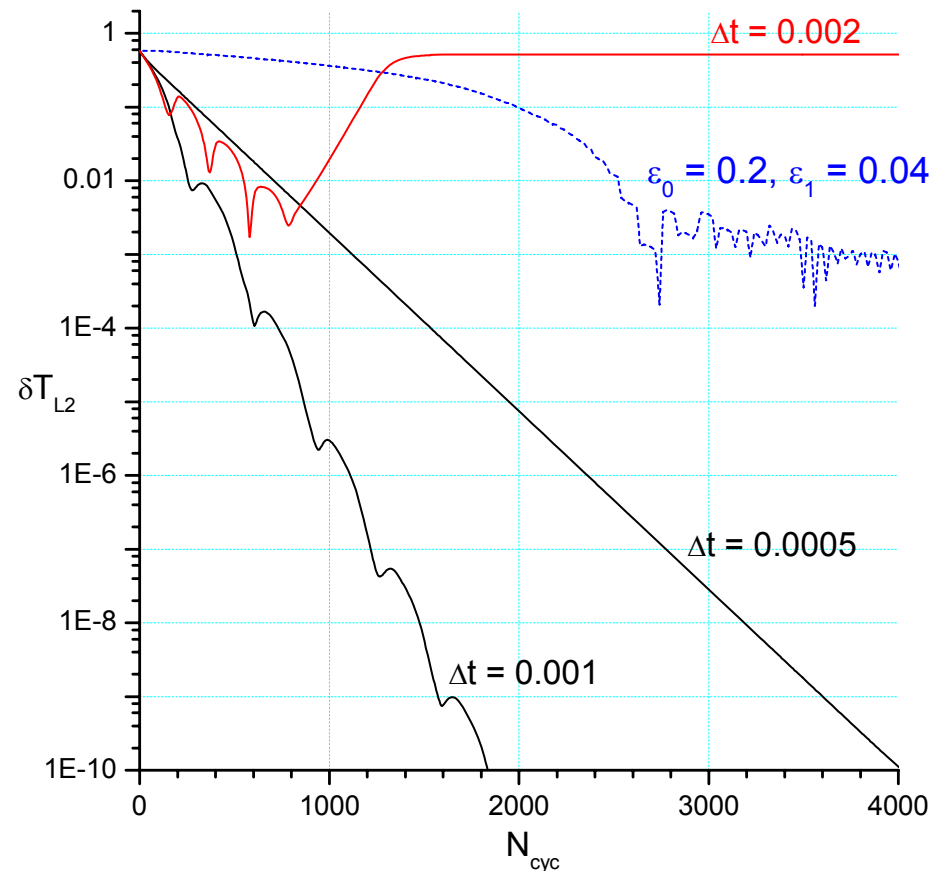
$$T(x, y) = x$$

is reproduced exactly on all grids, unless special constraints to ensure positiveness are imposed on *strongly distorted* grids.

For sufficiently large time steps Δt , the SSI method does not converge to the steady-state solution – an indication of its conditional stability (zero for large Δt).

Piecewise linear solutions with κ -jumps are reproduced exactly only with harmonic mean $\kappa_{f,ij}$, and only on rectangular grids.

Time convergence to the steady state



Test problems: non-linear wave into a cold wall

Parameters: $\rho c_v = 1, \quad \kappa = \kappa_0 T^3$

Initial condition: $T(0, x) = 0$

Boundary condition: $T(t, 0) = 1$

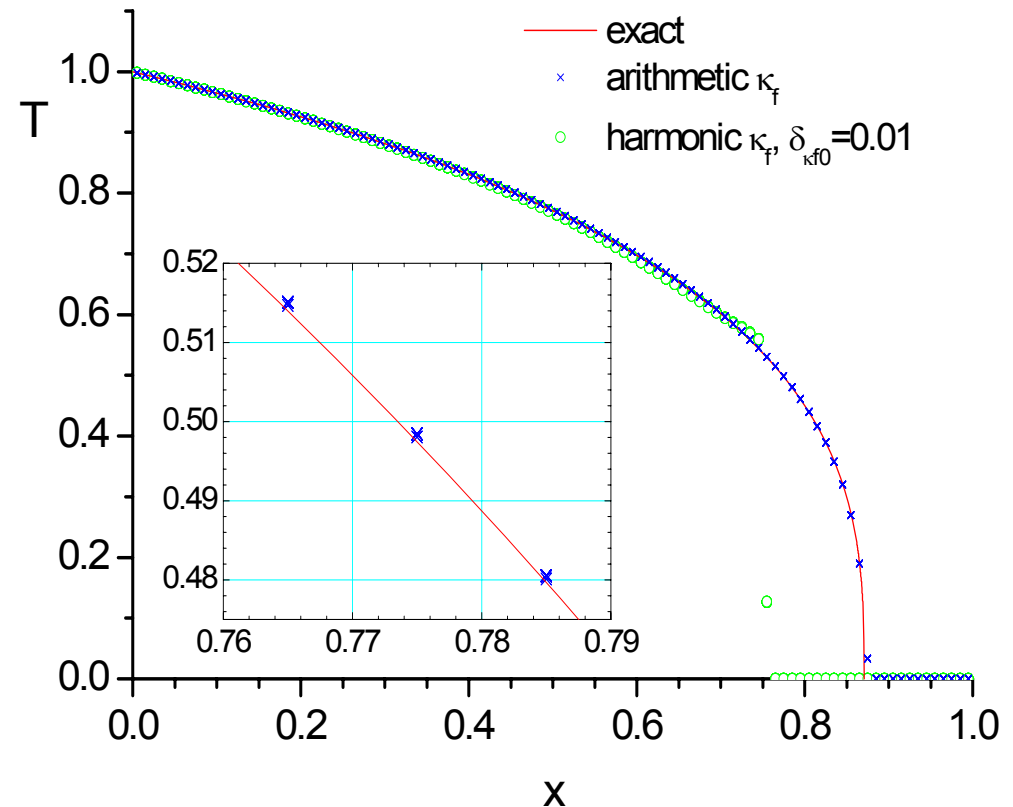
Solution: $T(t, x) = \tau(\xi), \quad \xi = \frac{x}{\sqrt{\kappa_0 t / 2}},$

$$\frac{d^2 \tau^4}{d\xi^2} + \xi \frac{d\tau}{d\xi} = 0$$

Test results:

This solution cannot be simulated with the harmonic-mean κ_f , whereas excellent results are obtained with the arithmetic-mean κ_f : the front position is reproduced with an error of 0.1% for $\varepsilon_0=0.2, \varepsilon_1=0.02$.

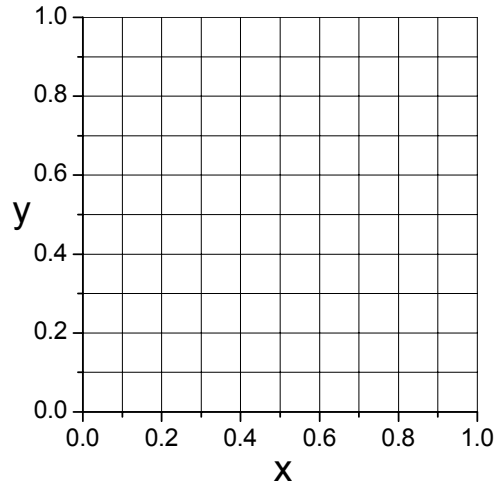
Square grid 100x100



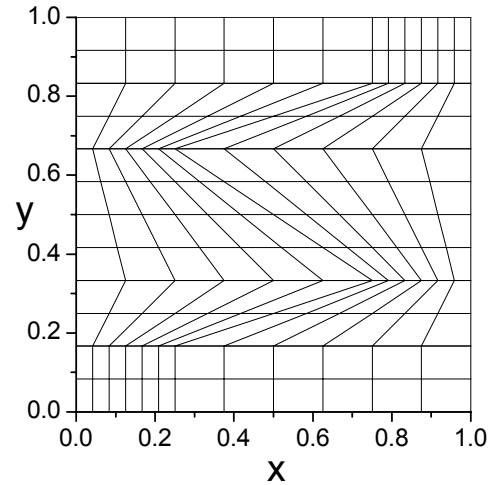
Temperature in all cells

Standard grids for test problems

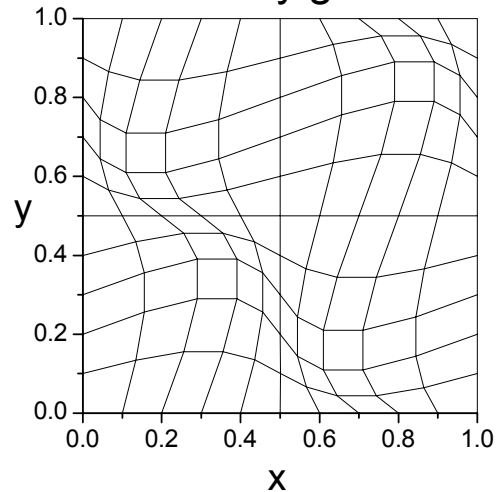
Square grid



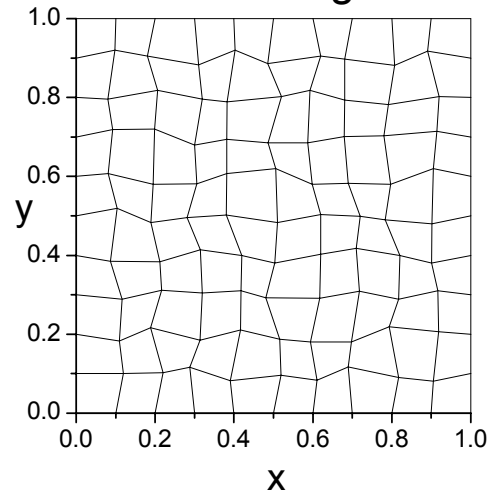
Kershaw grid



Wavy grid



Random grid



Only the Kershaw grid is *strongly* distorted in the sense that some of the coefficients $(1 \pm \xi)(1 \pm \eta)$ become negative.

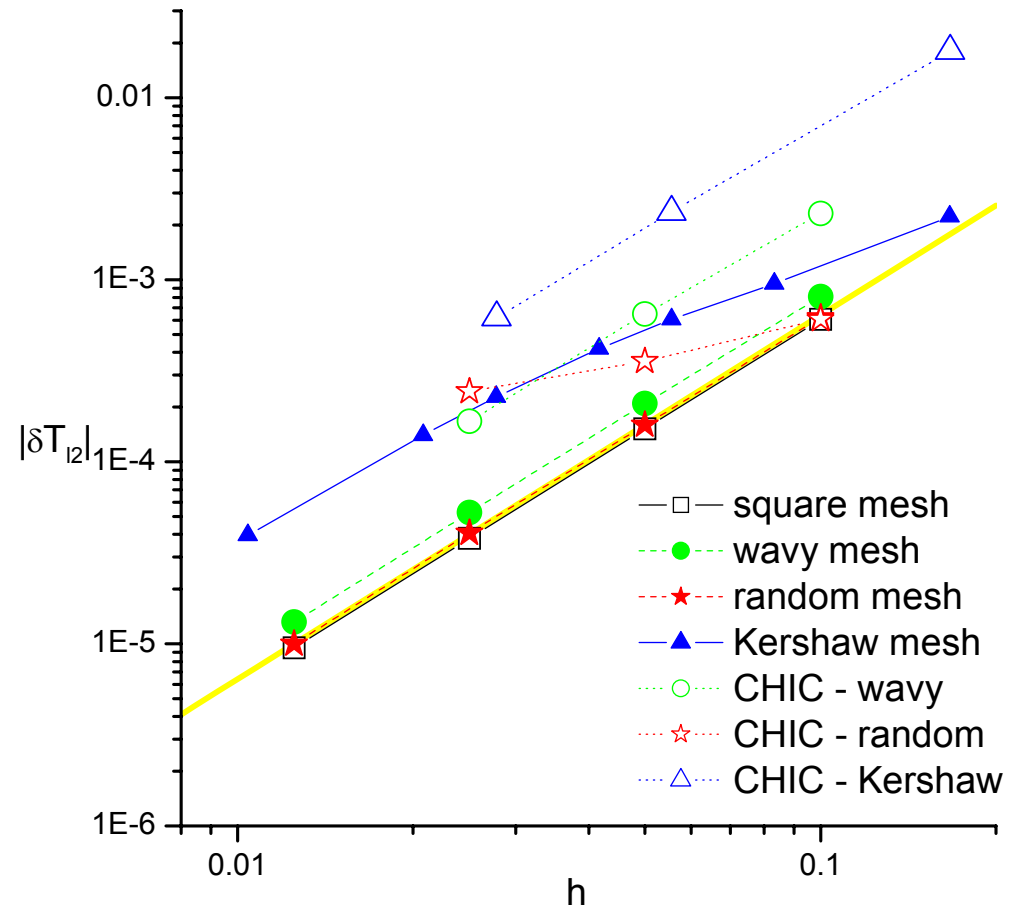
Test problems: non-linear steady-state solution

Here we test against a steady-state solution of the form

$$T(x, y) = a + bx + cx^4,$$

with the source term $Q = Q(x, y) = x^2$.

Our scheme clearly demonstrates the 2nd order convergence rate on all grids, and is no less accurate than the best published schemes of Morel *et al.* (1992), Shashkov *et al.* (1996), Breil & Maire (2007).



Test problems: non-linear wave into a warm wall

[originally proposed by E.Livne & A.Glasner (1985)]

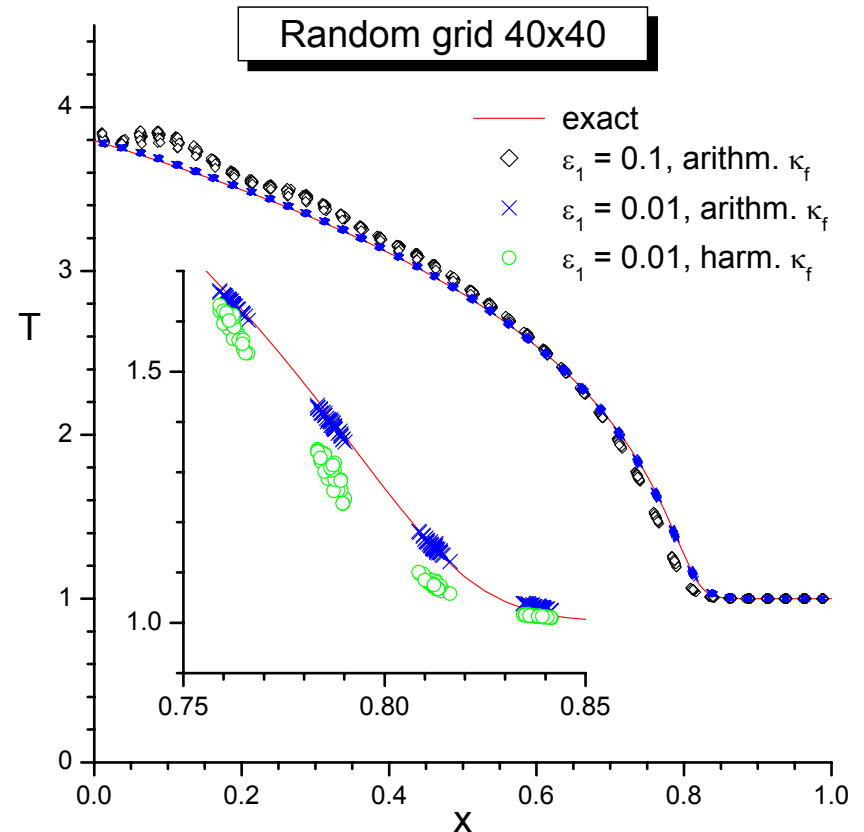
Parameters: $\rho c_V = 1, \quad \kappa = \kappa_0 T^4$

Initial condition: $T(t, x)_{t \rightarrow -\infty} = 1$

Solution: $T(t, x) = 1 + \phi(\xi), \quad \xi = \kappa_0^{-1}(t - x),$
 $\xi = \ln \phi + 4\phi + 3\phi^2 + \frac{4}{3}\phi^3 + \frac{1}{4}\phi^4$

Test results:

- For good accuracy we need “ghost” energy control, $\varepsilon_1 < 0.01-0.02$.
- Arithmetic-mean κ_f is by far more accurate than the harmonic-mean value.



Test problems: non-linear wave into a warm wall

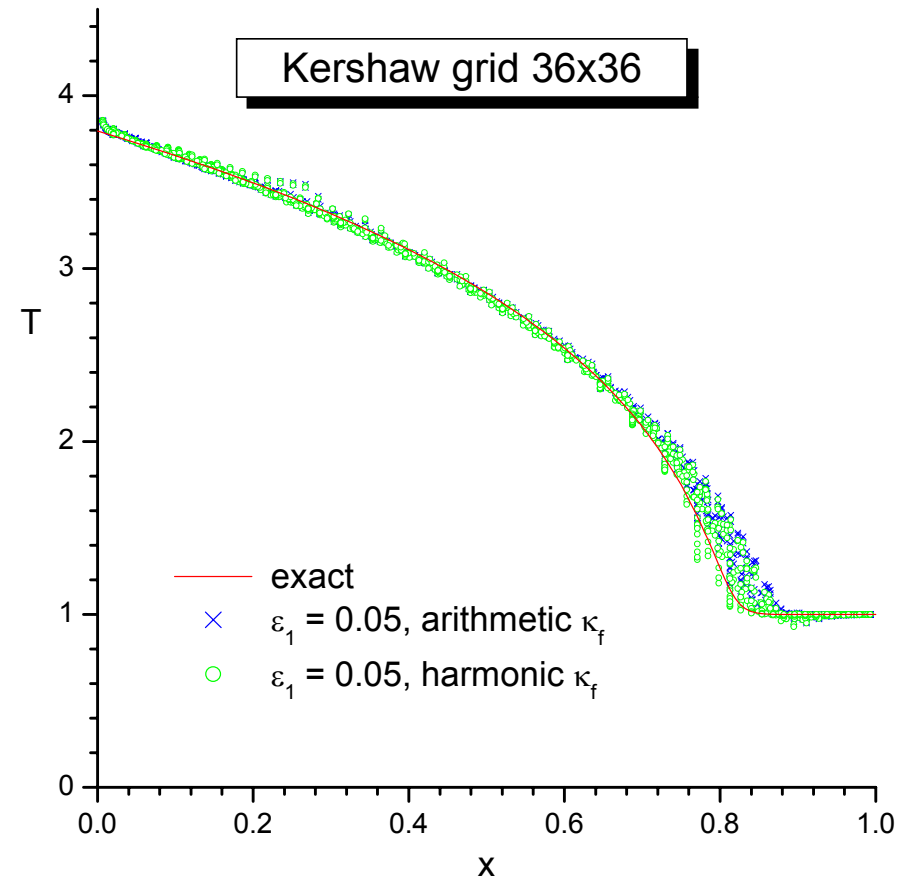
Parameters: $\rho c_v = 1, \quad \kappa = \kappa_0 T^4$

Initial condition: $T(t, x)_{t \rightarrow -\infty} = 1$

Solution: $T(t, x) = 1 + \phi(\xi), \quad \xi = \kappa_0^{-1}(t - x),$
 $\xi = \ln \phi + 4\phi + 3\phi^2 + \frac{4}{3}\phi^3 + \frac{1}{4}\phi^4$

Test results:

On *strongly distorted* grids both the arithmetic mean and the harmonic mean κ_f yield about the same accuracy.



Temperature in all cells

Diffusion test cases



- **Non linear thermal wave** on a distorted grid

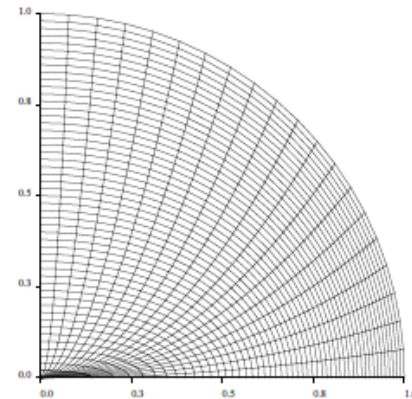
$$\rho C \frac{dT}{dt} - \nabla \cdot (\kappa(T) \nabla T) = 0,$$

with $\rho = 1$, $C = 1$, $\kappa(T) = T^{\frac{5}{2}}$ and $T^0 = 1$. Computational domain $(r, \theta) \in [0, 1] \times [0, \frac{\pi}{2}]$.

Distorted polar grid

$$x' = \sqrt{r} \cos \theta,$$

$$y' = r \sin \theta.$$

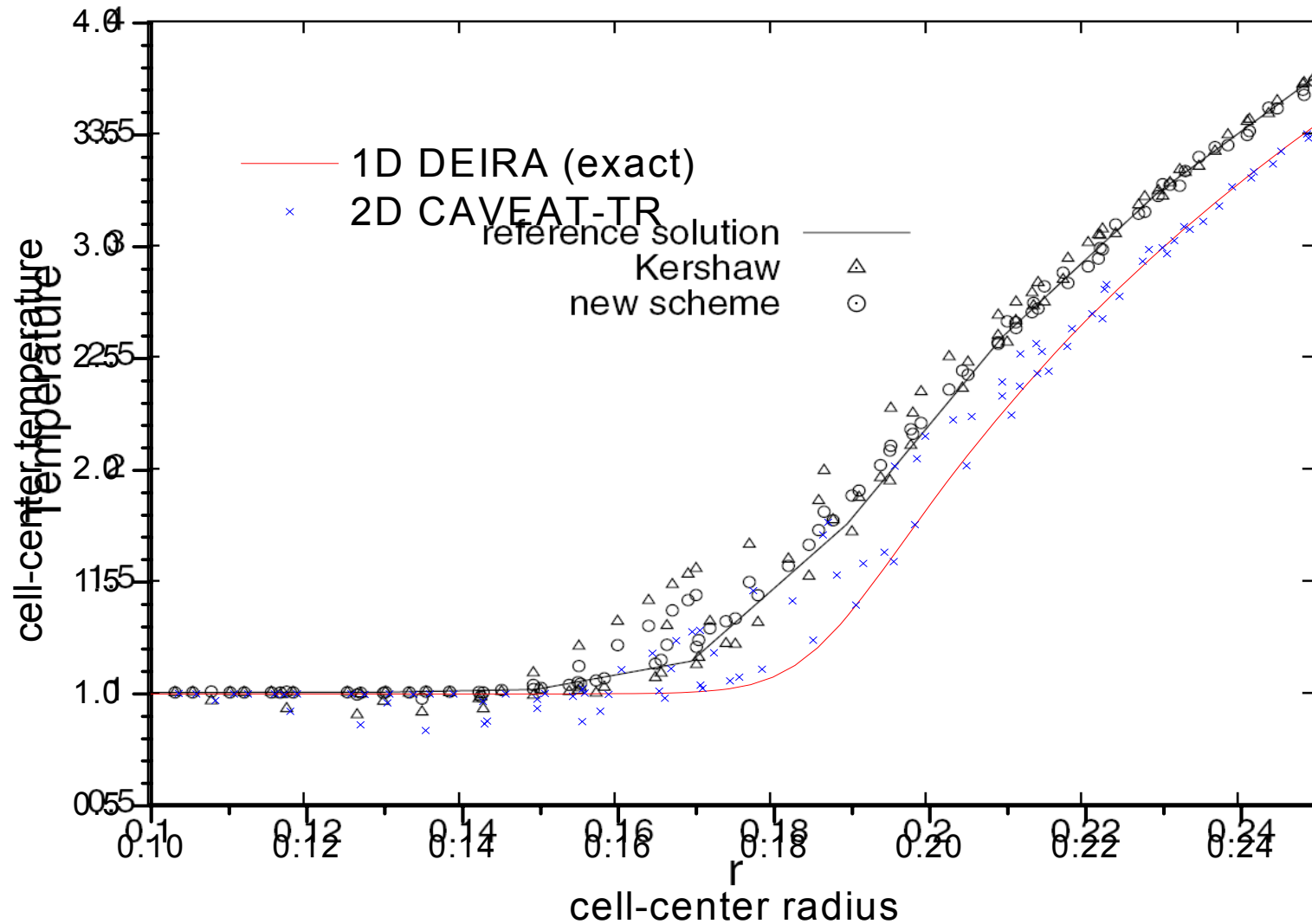


50 × 20 cells

Boundary conditions : $\Phi_{\text{ext}} = 10^3$ at the external radius.

Thermal conduction: comparison with CHIC

CHIC: fully implicit; **RALEF:** SSI – symmetric semi-implicit \Rightarrow faster and more accurate



Radiation transport

Neither the CHIC code nor the KIAM code have radiation transport, only multi- (single-) group diffusion.

Radiation transport: coupling to the fluid

Radiation coupling to the fluid is combined with thermal conduction within the unified SSI approach.

Partially implicit discretization of the fluid energy equation

$$M_{ij} (\bar{E}_{ij} - E_{ij}) = \left(\tilde{W}_{ij}^T + \tilde{W}_{ij}^r + W_{ij}^{dep} \right) \Delta t + W_{ij}^p \Delta t,$$

$$c_{V,ij} M_{ij} (\tilde{T}_{ij} - T_{ij}) = \left(\tilde{W}_{ij}^T + \tilde{W}_{ij}^r + W_{ij}^{dep} \right) \Delta t; \quad \tilde{W}_{ij}^r = W_{ij}^r + \frac{\partial W_{ij}^r}{\partial T_{ij}} (\tilde{T}_{ij} - T_{ij});$$

yields

$$\left(\tilde{W}_{ij}^T + \tilde{W}_{ij}^r + W_{ij}^{dep} \right) \Delta t = c_{V,ij} M_{ij} \frac{\left(W_{ij}^T + W_{ij}^r + W_{ij}^{dep} \right) \Delta t + \delta_{ij}^T + \delta_{ij}^r}{c_{V,ij} M_{ij} + \left(D_{ij}^T + D_{ij}^r \right) \Delta t},$$

$$D_{ij}^T = -\frac{\partial W_{ij}^T}{\partial T_{ij}}, \quad D_{ij}^r = -\frac{\partial W_{ij}^r}{\partial T_{ij}}.$$

In the SSI method we have to calculate the explicit cell heating power W_{ij}^r and its temperature derivative $D_{ij}^r = -\partial W_{ij}^r / \partial T_{ij}$.

Algorithm for radiation transport: general outline

The numerical algorithm for radiation transport splits into two parts:

- ❖ part 1: calculation of the intensity field $I_{ij}(\nu, \vec{\Omega})$;
- ❖ part 2: calculation of the cell heating power $W_{ij} = \int_{V_{ij}} dV \int_0^\infty \left(\int_{4\pi} I d\vec{\Omega} - 4\pi B_\nu \right) d\nu$
and its temperature derivative $D_{ij}^r = -\partial W_{ij}^r / \partial T_{ij}$.

In part 1 of the algorithm the exact solution of the transport equation across a quadrilateral cell with a fixed absorption coefficient $k_\nu = \text{const}$ is used; the interpolation scheme for the source function B_ν is of primary importance.

Even if the radiation field is calculated quite accurately, this is no guarantee for adequate coupling with the fluid in the diffusion limit!

Part 1: the method of short characteristics

- ❖ angular directions are discretized by using the **S_n method** with $n(n+2)$ fixed photon propagation directions over the 4π solid angle;
- ❖ for each angular direction $\vec{\Omega}_L$ and frequency ν , the radiation field I is found by solving the transfer equation

$$\vec{\Omega}_L \cdot \nabla I = k_\nu (B_\nu - I), \quad I = I(t, \vec{x}, \nu, \vec{\Omega}_L),$$

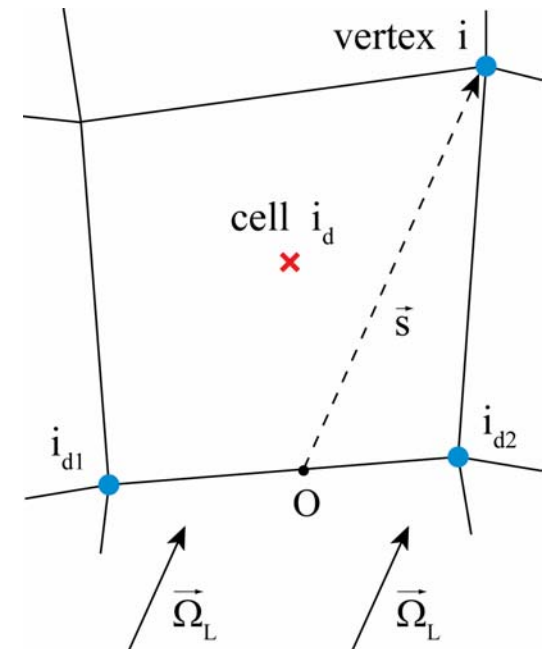
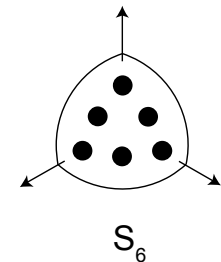
with the **method of short characteristics** (A.Dedner, P.Vollmöller, JCP, **178**, 263, 2002). **Mesh nodes** are chosen as collocation points for the radiation intensity I .

Advantages:

- even on strongly distorted meshes, it is guaranteed that light rays pass through each mesh cell;
- the algorithm is generally computationally more efficient than that of long characteristics.

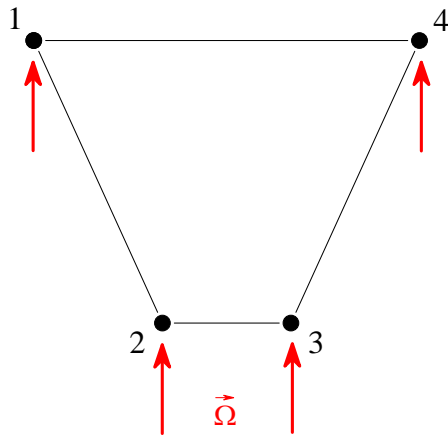
Disadvantages:

- a significant amount of numerical diffusion in space.



Flux conservation in vacuum

An important shortcoming of the vertex collocation points for radiation intensities is violation of the flux conservation in vacuum, where the transfer equation requires



$$\nabla \cdot (\vec{\Omega} I) = 0 \Rightarrow \oint_L (\vec{\Omega} \cdot \vec{n}) I dl = 0$$

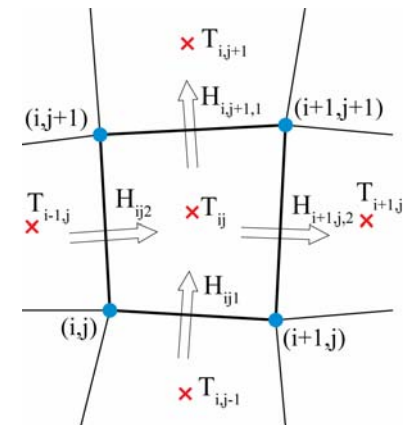
In our example on the left we have

$$H_{in} = \frac{1}{2}(I_1 + I_2)l + \frac{1}{2}(I_2 + I_3)l + \frac{1}{2}(I_3 + I_4)l$$

$$H_{out} = \frac{1}{2}(I_1 + I_4)l \neq H_{in}$$

Conclusion: we cannot adopt the same fluxing algorithm that was used for thermal conduction to calculate the radiative energy deposition

$$W_{ij}^r = H_{ij1} + H_{ij2} - H_{i,j+1,1} - H_{i+1,j,2}$$

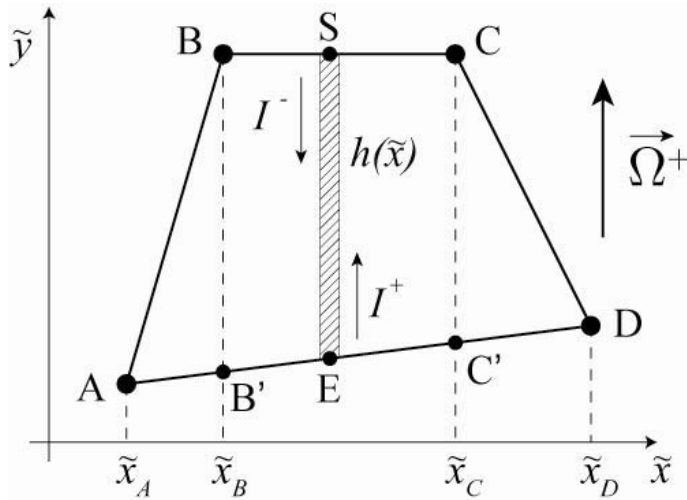


Our numerical scheme for radiation energy transport inevitably becomes non-conservative!

Conservativeness can be restored by assigning the intensity I to cell faces (R.Ramis, 1992).

Part 2: bidirectional cell integration

When calculating W_{ij}^r , propagation directions $\vec{\Omega}_L$ are combined in \pm pairs.



The cell heating power W_{ij}^r is calculated by integrating the column heating power

$$W_h = (F_E^+ + F_S^-) (1 - e^{-\tau_h}) + \phi_3(\tau_h) (B_S - B_E) / \tau_h,$$

$$F^\pm = I^\pm - B, \quad \phi_3(x) = x - 2 + (x + 2)e^{-x},$$

$$\tau_h = k_\nu h(\tilde{x}).$$

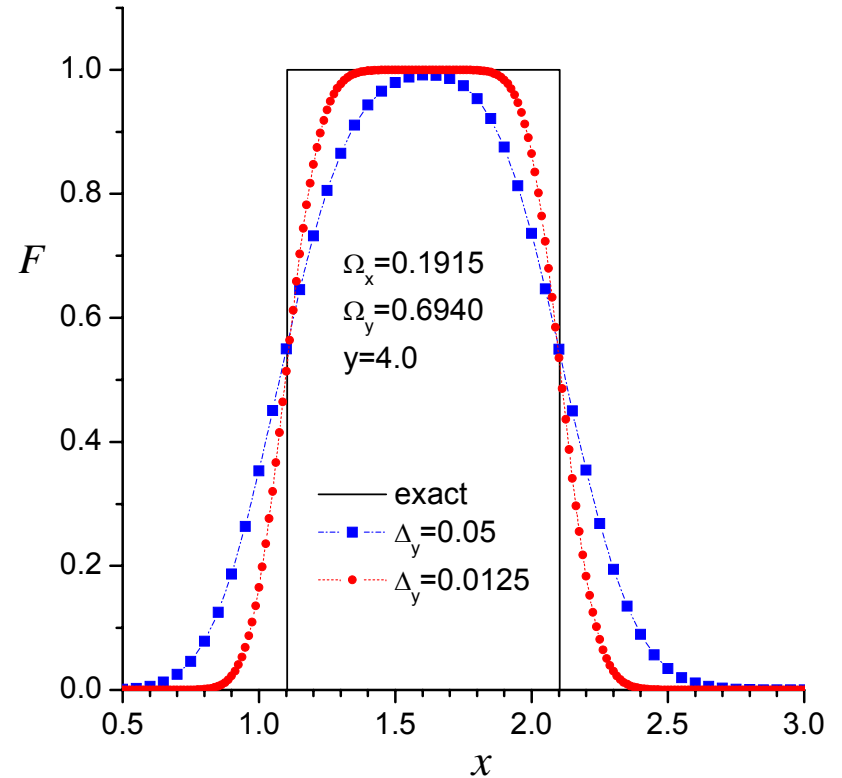
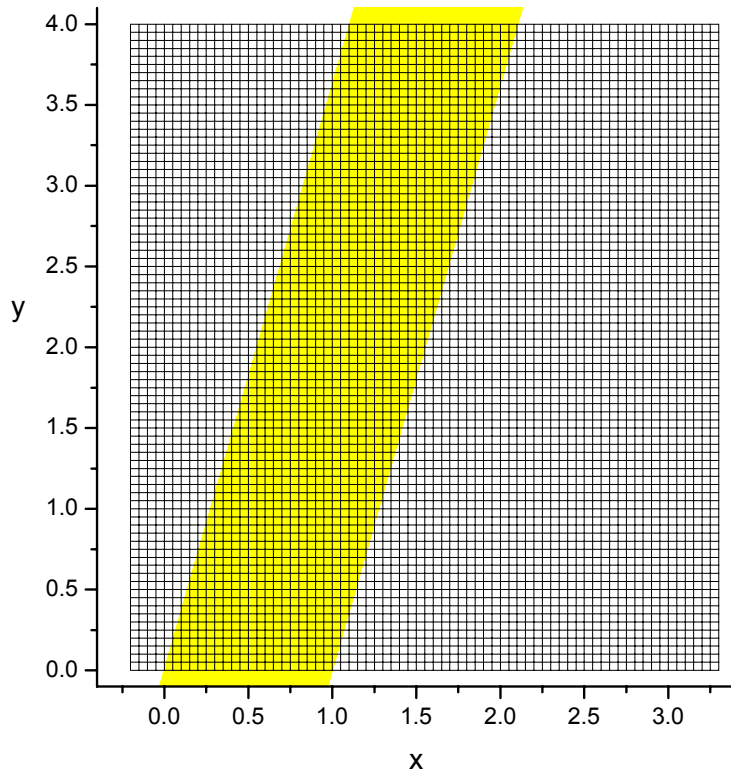
After we employ a second-order (parabolic) interpolation for the source function $B(\tau)$ along the light rays, we do recover the diffusion limit for $\tau \gg 1$, where

$$Q_r = \text{div} \left(\frac{4\pi}{3k_{\text{Ross}}} \nabla B \right)$$

Radiation transport: test problems

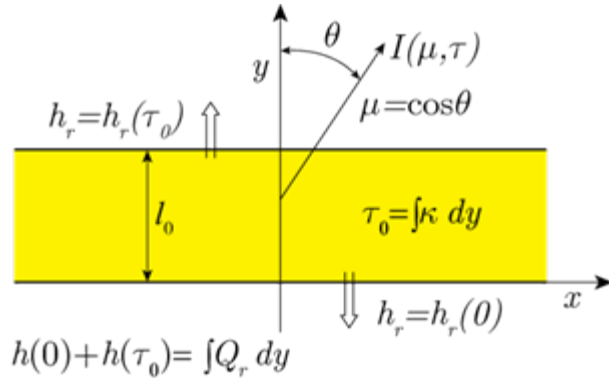
Numerical diffusion: a searchlight beam in vacuum

The short-characteristic method produces a significant amount of numerical diffusion for light beams with sharp edges.

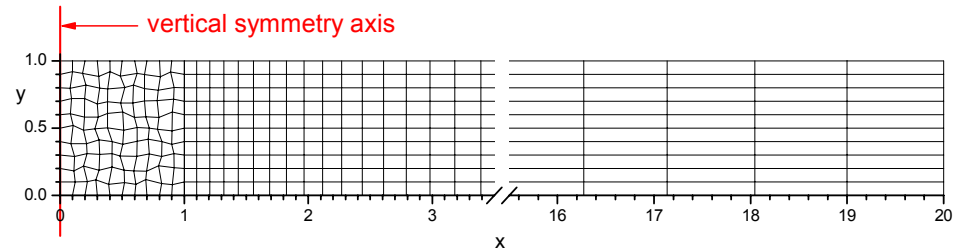


For thermal radiation a certain amount of numerical diffusion may be more an advantage than a drawback.

Test problems: radiative cooling of a slab



Computational mesh:



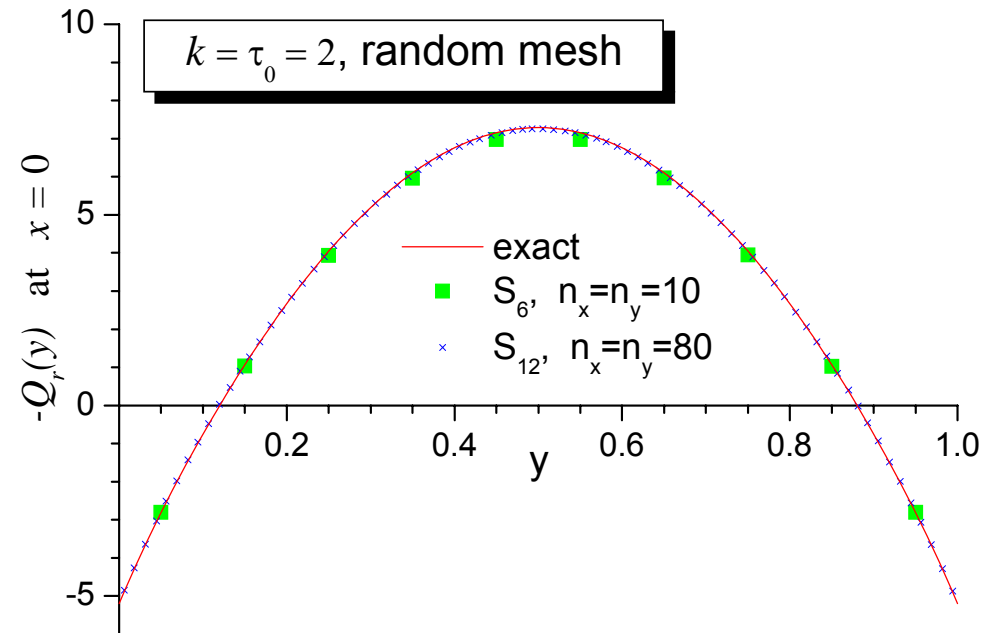
Exact solution:

$$\mu \frac{\partial I}{\partial y} = k_0 (B - I), \quad B(y) = \sin(\pi y), \quad 0 \leq y \leq 1;$$

$$Q_r(y) = 2\pi k_0 \left[k_0 \int_0^1 B(y') E_1(k_0 |y - y'|) dy' - 2B(y) \right];$$

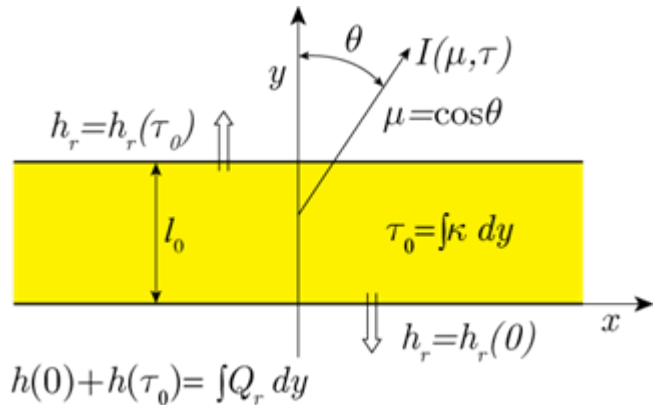
Convergence of the S_n method

	S_2	S_4	S_6	S_8	S_{12}
error L_2	23%	7.6%	2.3%	1.9%	1.15%



Typical accuracy in problems with optically thin mesh cells is 1–2%.

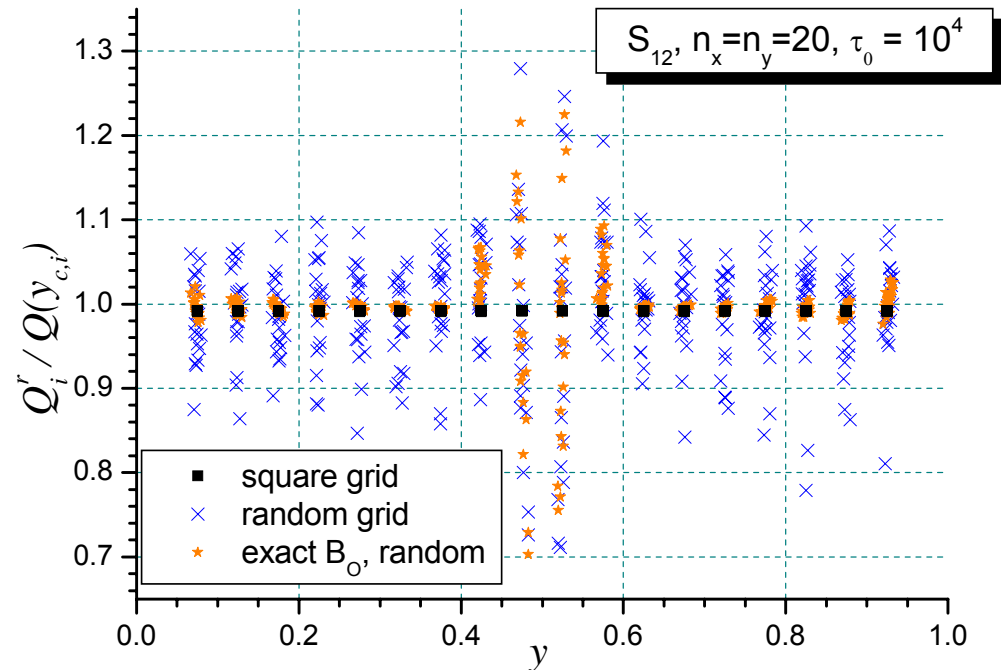
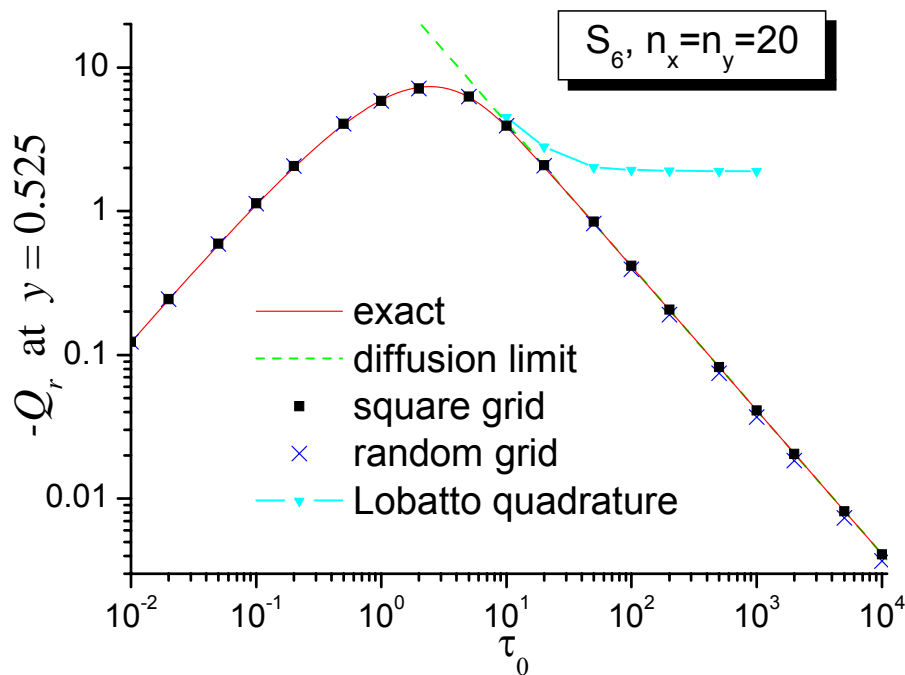
The diffusion limit



At $\tau_0 \gg 1$ one approaches **the diffusion limit**.

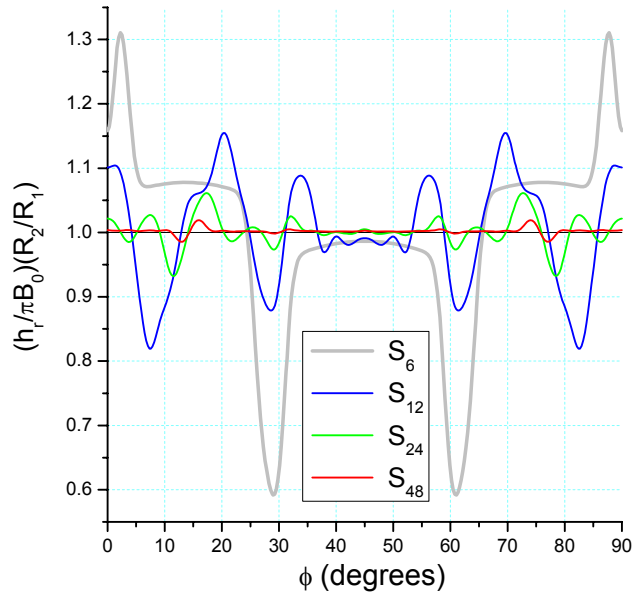
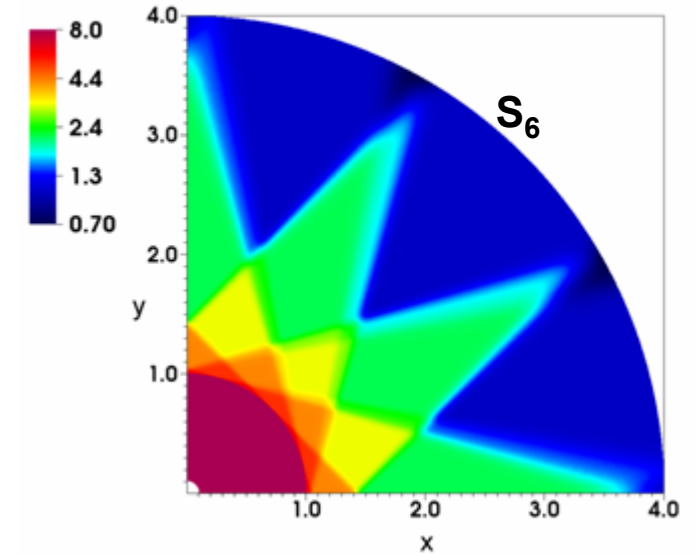
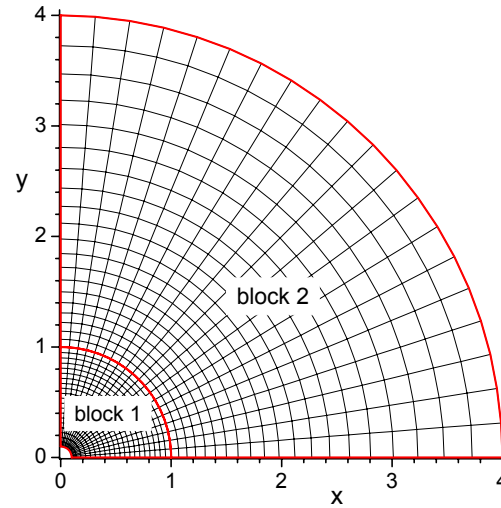
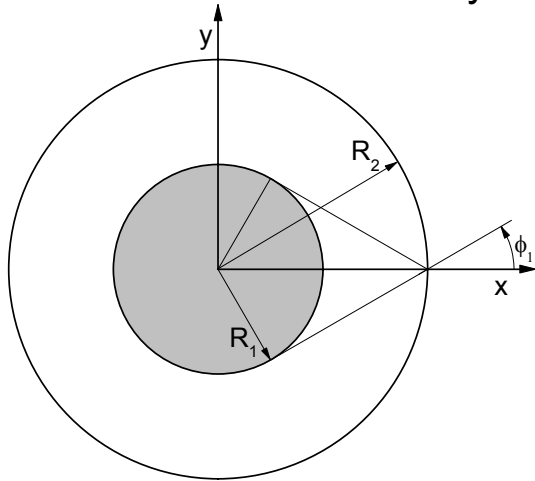
Many transport codes fail to reproduce the energy exchange rate Q_r in the diffusion limit.

The RALEF-2D algorithm remains robust for mesh cells of arbitrary optical thickness; in the limit of $\tau_0 \rightarrow \infty$ it produces a finite numerical error.



The “ray effect” in a cylindrical cavity

Consider radiation transport from a central “hot” rod across a vacuum cavity.



Convergence of the S_n method

$R_2/R_1=4$	S_6	S_{12}	S_{24}	S_{48}	S_{96}
error max/min	41%	18%	6.8%	1.9%	0.47%
error L_2	15%	8.5%	2.4%	0.52%	0.23%

EOS and opacities

EOS options in RALEF-2D

The principal scheme for different EOS options has been inherited from CAVEAT:

- ❖ one can define up to 30 different materials;
- ❖ for each material one can choose out of 9 different types of EOS.

The EOS model must provide

$$p = p(\rho, e), \quad c^2 = c^2(\rho, e), \quad T = T(\rho, e), \quad c_V = c_V(\rho, e), \quad z = z(\rho, e), \quad a_{Du} = a_{Du}(\rho, e).$$

Analytical EOS models:

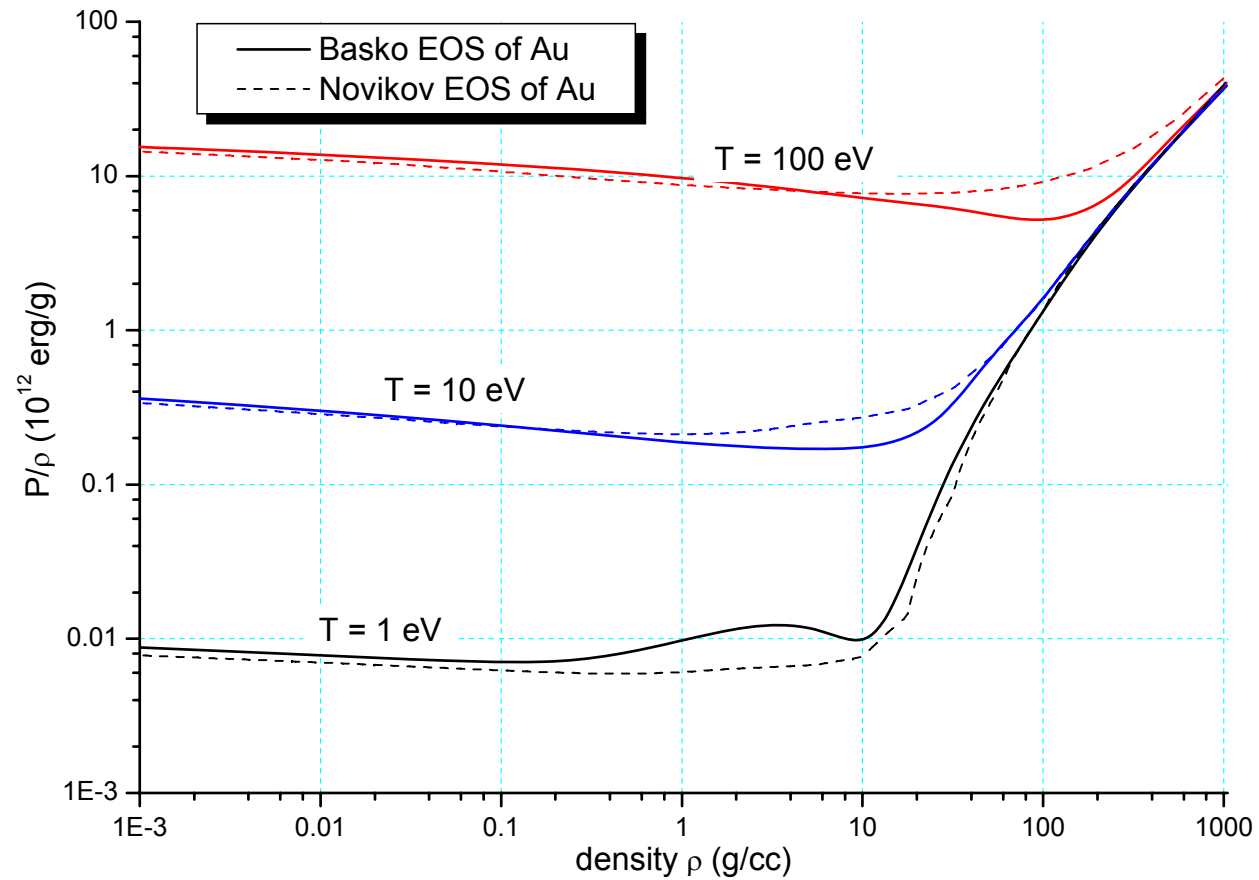
1. polytropic gas: $p = (\gamma - 1)\rho e$, $e = c_V T$, $a_{Du} = \frac{1}{2}(\gamma + 1)$, $c_V, z = const$
2. linear EOS: $p = (\rho - \rho_0)[c_1\rho_0 + c_2|\rho - \rho_0|] + (c_3\rho_0 + c_4\rho)e$, $T = (e - e_{cold})/c_V$, ...

Tabular EOS models:

7. general logarithmic-table (GLT) EOS with different source EOS models: Basko (Z = 1—13, 18, 22,26,28,29,36,40,42, 47 54,55,74,79,82,83,92), Novikov (THERMOS code; Z=1,6,13,22,29,74,79);
8. SESAME tabular EOS.

Basko vs Novikov source EOS

In some cases the Maxwell construction is possible for the Novikov EOS.

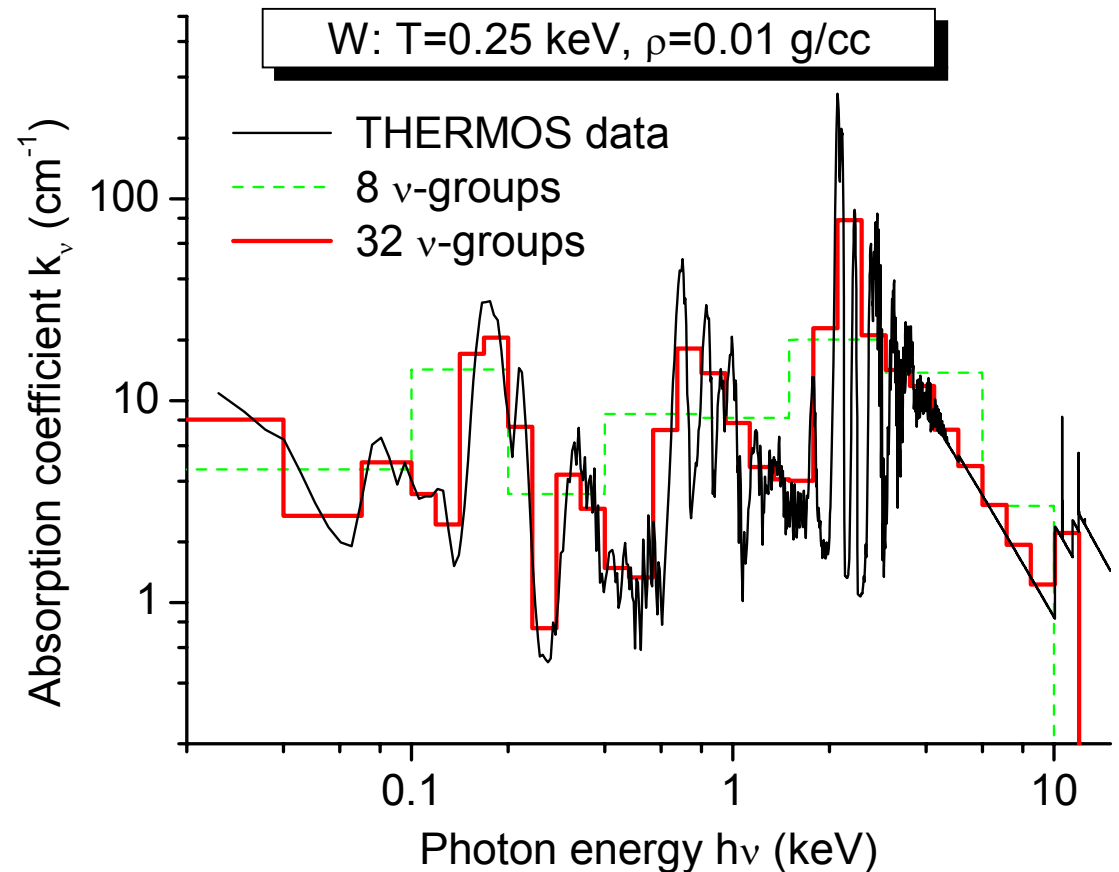


Opacity options in RALEF-2D

Here we profit from many years of a highly qualified work at KIAM (Moscow) in the group of Nikiforov-Uvarov-Novikov (the THERMOS code based on the Hartree-Fock-Slater atomic modeling).

Opacity options:

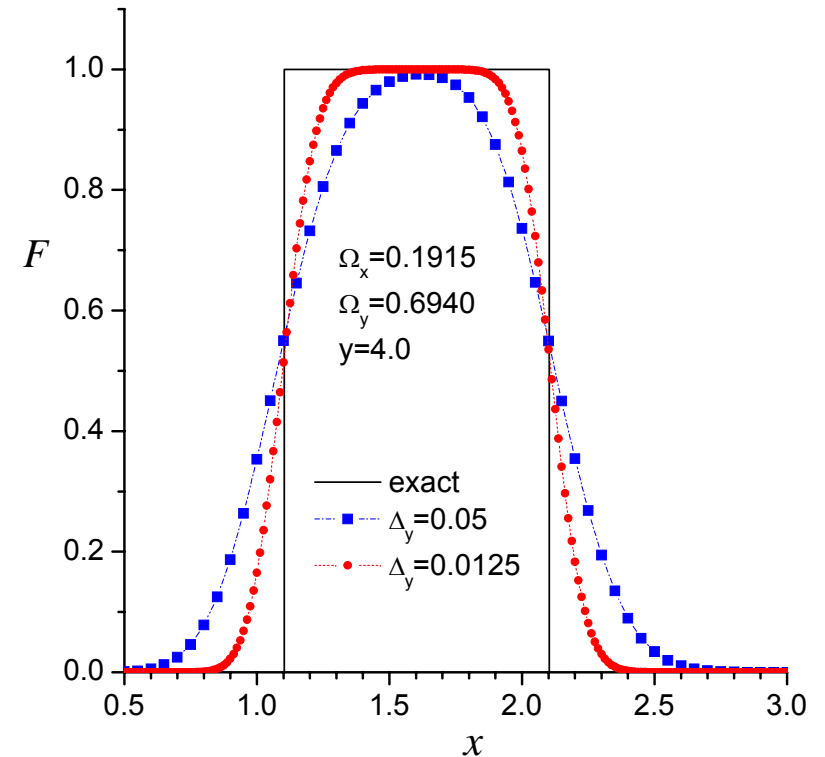
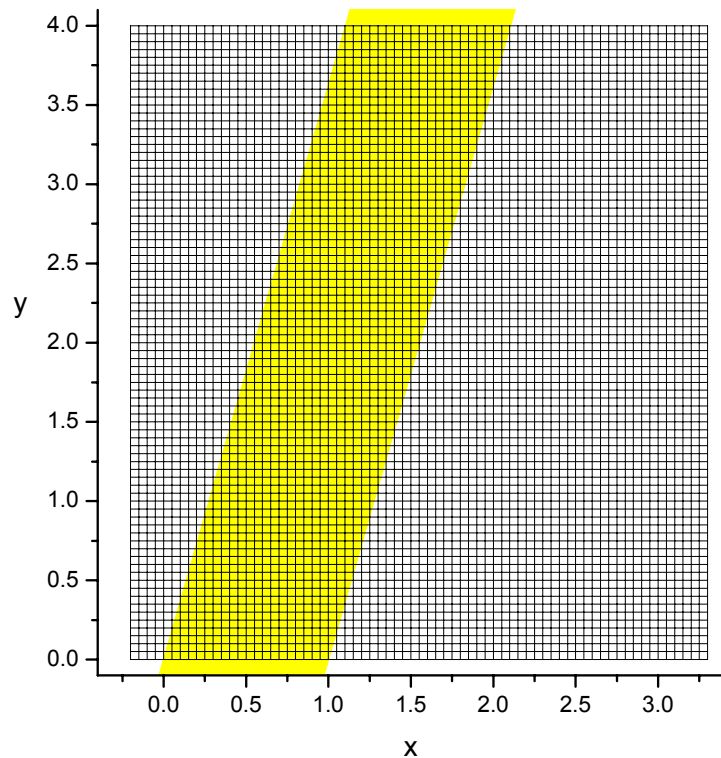
1. power law,
2. ad hoc analytical,
3. inverse bremsstrahlung (analytical),
-
7. GLT tables (source opacities from Novikov)



Laser absorption

Laser absorption in RALEF-2D

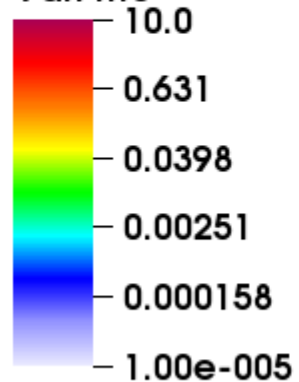
- Present model:**
- ❖ one laser beam treated by the same method of short characteristics as the radiation transport;
 - ❖ no refraction, the inverse bremsstrahlung absorption coefficient, 100% absorption at the critical surface.



DB: vtkall001.vtk
Cycle: 2039 Time: 0.1

Pseudocolor

Var: rho



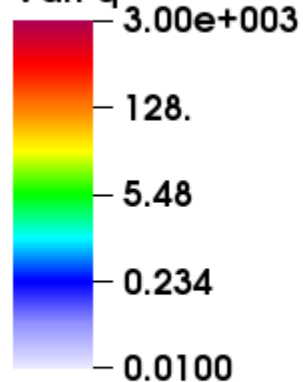
Max: 23.6

Min: 9.89e-006

y (mm)

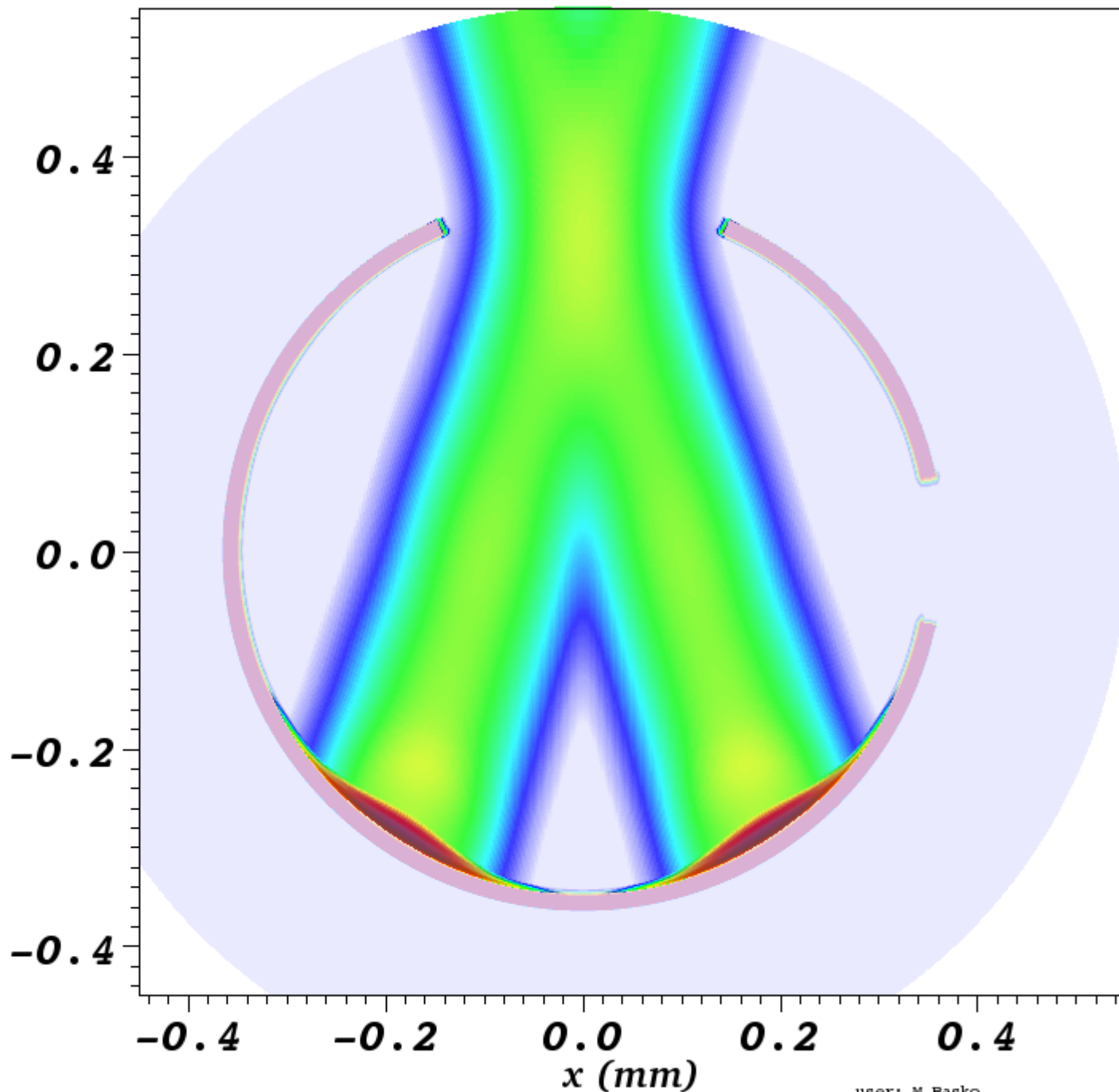
Pseudocolor

Var: q



Max: 4.61e+003

Min: 0.000



Summary

- ❖ It appears that the RALEF-2D code has good chances to be recognized as one of the most powerful in its class in terms of speed, accuracy and variety of solvable problems.

- ❖ Further work is needed
 - 1) to implement radiation transport in the axially symmetric r-z geometry,
 - 2) to improve the laser absorption model,
 - 3) to improve the 2nd order remapping algorithm,
 - 4) to improve the algorithm for Lagrangian node velocities.